PERGAMON

Journal of Steroid Biochemistry & Molecular Biology 72 (2000) 125–132

The Journal of Steroid Biochemistry & Molecular Biology

www.elsevier.com/locate/jsbmb

Vitamin D receptor interactions with positive and negative DNA response elements: an interference footprint comparison

Nicholas J. Koszewski[a,*], Hartmut H. Malluche[a], John Russell[b]

[a] *Division of Nephrology, Bone and Mineral Metabolism, Department of Internal Medicine, University of Kentucky Medical Center, Lexington, KY 40536, USA*

[b] *Department of Medicine, Albert Einstein College of Medicine, Bronx, NY 1002, USA*

Received 7 April 1999; accepted 9 October 1999

Abstract

Interference footprinting protocols were utilized to examine the interactions of the vitamin D receptor (VDR) with either a positive or a negative vitamin D response element (VDRE). A sequence from the human osteocalcin (hOC) gene was chosen for the prototypical positive DR + 3 VDRE, while an analogous sequence linked to the avian parathyroid hormone gene (aPTH) was used as the negative VDRE. Both types of response elements were examined for phosphate backbone contacts, as well as base-specific interactions with guanine and thymine residues. Sources of VDR included partially purified canine intestinal preparations, as well as extracts of recombinant human VDR and retinoid X receptor α prepared from baculovirus-infected Sf9 insect cells. Cold competition experiments using variable amounts of these oligonucleotides in the mobility shift assay revealed that the hOC element was a five-fold better competitor for heterodimer complex binding than the negative VDRE. Interference footprints revealed extensive strong contacts to the phosphate backbone and individual guanine and thymine nucleotides of the hOC element. The composite hOC footprint was asymmetric for the number and strength of interactions observed over each of the respective direct repeat half-sites. In contrast, the aPTH VDRE footprints revealed fewer points of DNA contact that were limited to the hexanucleotide repeat regions and were strikingly weaker in nature. The alignment of DNA contact points for both elements produced a 5′ stagger that was indicative of successive major groove interactions, and consistent with dimer binding. DNA helical representations indicate that the heterodimer contacts to these response elements are substantially different and provide insight into functional aspects of each complex.

1. Introduction

The VDR, like other members of the steroid receptor superfamily, binds to discrete sequences of DNA to alter transcriptional events in a ligand-dependent manner [1,2]. The classical VDRE consists of two hexanucleotide direct repeats separated by three intervening base-pairs (DR + 3) [3–9], yet despite the strong homology that exists between the DR + 3 VDREs, significant deviations can be observed between elements, as well as between individual half-sites that comprise an element.

In an earlier study, the identification of a VDRE near the promoter of the chicken parathyroid hormone gene was reported [10]. This sequence was able to convey hormone-dependent down-regulation of gene expression in a mammalian cell line when linked to either the native or a heterologous promoter. Comparisons with other known positive vitamin D response elements indicated that this negative element fell into the same DR + 3 format that characterizes other vitamin D receptor binding sites. The only notable deviation from the positive elements occurred in the final two nucleotides of the 3′ half-site of the aPTH direct repeat, GGGTCAGGAGGGTGT, that ends with a GT dinucleotide rather than the more typical CA.

* Corresponding author. Tel.: +1-606-323-6502; fax: +1-606-323-0232.

E-mail address: njhosz0@pop.uky.edu (N.J. Koszewski).

0960-0760/00/$ - see front matter
PII: S0960-0760(00)00022-4

An earlier study, which used partially purified canine intestinal receptor preparations as a source of VDR [10], found that the phosphate interference footprint over the avian element produced a weak set of contact points. The limited number of reports using methylation interference protocols suggested that the VDR contacts to positive VDREs may be inherently different than that observed with the negative aPTH element [4,11–13]. In the present study, a more comprehensive interference footprinting comparison between a prototypical, naturally-occurring, positive VDRE from the hOC gene [4,14] and the aPTH sequence was undertaken. Canine intestinal receptor preparations, a tissue known to possess elevated concentrations of the receptor [15], as well human recombinant proteins derived from baculoviral infection of insect cells were used and compared for their ability to interact with these elements. The results demonstrate that there is a good correspondence in the footprints generated from the intestinal and recombinant sources of receptor. In addition, the data indicate that the interference profile is drastically altered, depending on the unique DNA sequence of the response element. This finding suggests that the contact points between the heterodimer complex and the individual DNA sequence may play a role in the underlying mechanism for the positive and negative transcriptional responses mediated through each DNA element.

2. Methods

2.1. General

All enzymes were purchased from New England Biolabs (Beverly, MA). γ-^{32}P-ATP (6000 Ci/mmol) and α^{32}P-dATP (3000 Ci/mmol) were purchased from Dupont NEN Research Products (Wilmington, DE). Oligonucleotides were synthesized at the University of Kentucky Molecular Structure Analysis Facility. The pHOC11 plasmid has been described previously [10,13], and fragment excision was accomplished by the combination of HindIII and EcoRI restriction enzymes to liberate a 77 bp fragment (hOC). The aPTHpG7 plasmid was generated by annealing a 30 bp oligonucleotide consisting of 5′ GGGTGGGCACATGAGGGTCAGGAGGGTGTG and cloning into the EcoRI site of pGEM7zf. The combination of ApaI and HindIII restriction enzymes generates an 88 bp fragment (aPTH). Recombinant proteins obtained from baculovirus infection of Sf9 cells and partially purified canine intestinal extracts were prepared as described previously [10,13]. 1,25-Dihydroxyvitamin D_3 was a generous gift from Dr. R. Horst, National Animal Disease Center (Ames, IA). The 9A7γ anti-VDR monoclonal antibody was a generous gift from Dr. J. W. Pike, University of Cincinnati (Cincinnati, OH), while Ab192 has been described previously [16]. The anti-RXRα antiserum used in the Western blot protocol was a generous gift from Dr. D. Noonan, University of Kentucky (Lexington, KY), while the anti-RXRα and RXRγ polyclonal antibodies used in the mobility shift assay were purchased from SC Biotech (Santa Cruz, CA).

2.2. Electrophoretic mobility shift assays

DNA probes were generated by endlabeling linearized and CIP-treated plasmids with polynucleotide kinase. Typically, 10–15,000 cpm of probe (ca. 3–5 fmol) were mixed with the protein extracts for the gel mobility shift assay. Preparation and binding conditions for the partially purified canine intestinal extracts were described previously [10], and consisted of 20 mM Tris (pH 7.5), 1.5 mM EDTA, 2 mM DTT, 120 mM KCl, 0.05% NP-40, 5% glycerol, 5.0 μg dIdC, 70 nM 1,25$(OH)_2D_3$ and 0.5 mM leupeptin in a total volume of 20 μl. Preparation and binding conditions for the recombinant proteins have been described previously [13]. Briefly, cytosols of recombinant human VDR (hVDR) or retinoid X receptor α (hRXRα) were diluted (1:25) in ice-cold KTEDG buffer (400 mM KCl, 20 mM Tris (pH 7.5), 1 mM EDTA, 2 mM DTT and 10% glycerol) prior to use. Samples were kept cold and 1 μl of each diluted extract was used in a 20 μl final volume in a buffer that included 120 mM KCl, 20 mM Tris (pH 7.5), 1.5 mM EDTA, 2 mM DTT, 5% glycerol, 0.5% CHAPS, 10 mM NaF, 100 μM Na_3VO_4, 1.0 μg dIdC and 100 nM 1,25-$(OH)_2D_3$. After incubation on ice for 30 min, the radiolabeled probe was added and incubation continued for 30 min. The samples were then applied to cooled, pre-run 5% polyacrylamide gels (29:1) in 0.5X TBE buffer and separated by electrophoresis at 14 V/cm for 2.5–3 h. Gels were transferred and dried and autoradiography was performed. Control serum or other antisera were added to the binding reaction prior to radiolabeled probe addition and allowed to incubate with the samples for 30 min before probe addition.

Cold competition binding reactions were carried out with annealed oligonucleotide competitors: hOC, 5′ CTAGATTGGTGACTCACCGGGTGAACGGGGGCATTGCG; aPTH 5′ CTAGAATGAGGGTCAGGAGGGTGTGCTGG; a 5′ mutated aPTH sequence (5′ mutaPTH), 5′ CTAGAGAGCCTCAGGAGGGTGTGCG; and the chicken vitellogenin perfect estrogen response element (cvitERE), 5′ GATCCCTGGTCAGCGTGACCGGAG. For the relative competitive binding experiments, the unlabeled competitor oligonucleotides were mixed with the radiolabeled aPTH probe before being added to the binding reaction.

2.3. Ethylation interference footprinting

The ethylation interference footprint experiments were performed as previously described [13,17,18]. Briefly, ^{32}P-endlabeled DNA probes in 50 mM sodium cacodylate buffer (pH 8.0) were treated with ethylnitrosourea-saturated ethanol for 20 min at 55°C. After precipitation with sodium acetate/ethanol and reprecipitation (3×), the pellets were washed with 70% ethanol, dried and resuspended in water. Ethylated probes were then used in the gel mobility shift assay as described above, except the amounts of probe which were increased to 10–15 fmol. Following electrophoresis, the wet gels were exposed to X-ray film overnight at 4°C. Acrylamide sections corresponding to bound and free DNA were excised, and the DNA was recovered by electrochemical elution and precipitation. Cleavage of the modified DNA was accomplished by treating it with 100 mM NaOH/0.1 mM EDTA in 10 mM phosphate buffer at 95°C for 30 min followed by neutralization with 3 M sodium acetate (pH 5.2) and precipitation with ethanol. Alternatively, the recovered ethylated probes were resuspended in 10% piperidine, heated at 95°C for 30 min, then dried in a rotary evaporator as described previously [18,19]. Samples processed by either method were separated through 10% sequencing gels, dried and autoradiography performed.

2.4. Thymine interference footprinting

The modification of thymine residues was carried out as previously described [20]. Briefly, radiolabeled DNA was dissolved in 5 μl of 30 mM Tris (pH 8.0), denatured at 95°C for 2 min and placed on wet ice. A 0.25 mM solution of potassium permanganate (20 μl) was added, and the sample was incubated at room temperature for 10 min. Then, 25 μl of stop solution (1.5 M sodium acetate/1.0 M β-mercaptoethanol) was added followed by 50 μl of water and five volumes of absolute ethanol to precipitate the DNA. The sample was reprecipitated and the pellet washed once with 95% ethanol. The dried pellet was resuspended in hybridization buffer (10 mM Tris (pH 8.0), 1 mM EDTA and 30 mM NaCl), followed by heating at 65°C for 5 min and slow cooling to room temperature. The recovered DNA was then used in the mobility shift assay and bound and free material recovered as described above. The recovered samples were treated with 10% piperidine at 95°C for 30 min and dried in a rotary evaporator. The pellet was resuspended in water and dried additionally three times prior to sequencing gel analysis.

2.5. Western blotting

The protein samples were separated on 10% gels, transferred onto polyvinylidenefluoride membranes and blocked for 30 min at 4°C with 1% nonfat dry milk in PBS/0.5% Tween 20. Incubation with the anti-VDR 9A7γ monoclonal antibody (1:10,000 dilution) or anti-RXRα antiserum (1:10,000) was continued in the same buffer overnight with gentle agitation. The blot was washed 3 × 10 min with PBS/Tween and then incubated with horseradish peroxidase-linked secondary antibodies (1:10,000 dilution). Following three washes as described above, the blotted proteins were

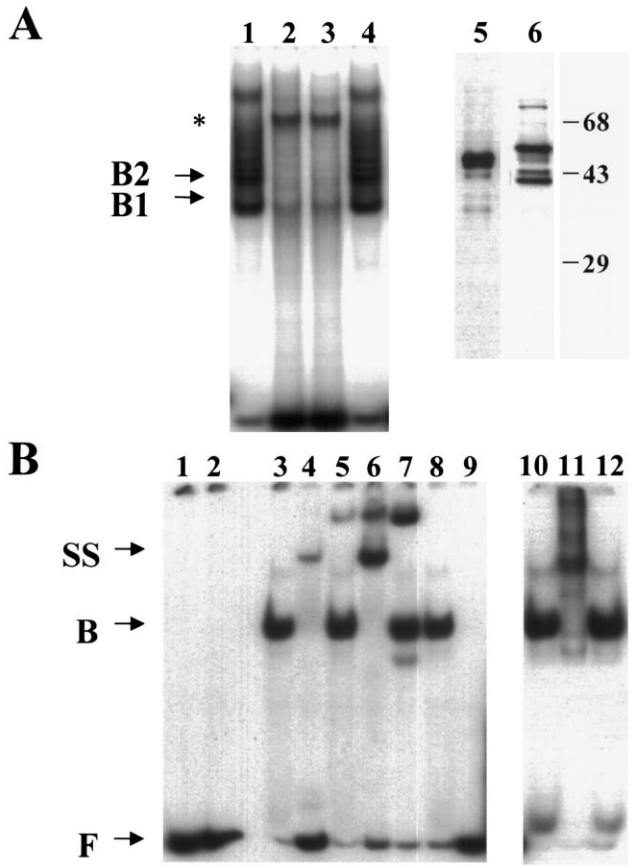

Fig. 1. Analysis of canine and recombinant proteins interacting with the hOC VDRE. (A) Partially purified canine intestinal extract was used as the source of protein for binding to the hOC VDRE (lanes 1–4). Lane 1, control binding reaction; lane 2, inclusion of 9A7γ anti-VDR antibody; lane 3, 200-fold excess of unlabeled hOC oligonucleotide; lane 4, 200-fold excess of cVitERE. Western blots of partially purified canine intestinal extract (lanes 5 and 6). Lane 5, VDR Western blot with immunoreactive protein observed at 50 kD; lane 6, RXRα Western blot with predominate immunoreactive protein observed at 55 kD and others appearing at 43 and 41 kD. Molecular weight markers in kilodaltons are indicated to the right. (B) Evaluation of recombinant proteins binding to the hOC VDRE. Lane 1, hVDR extract alone; lane 2, hRXRα extract alone; lane 3, combination of extracts; lane 4, inclusion of rat 9A7γ anti-VDR antibody; lane 5, control rat serum; lane 6, inclusion of Ab192 anti-VDR antiserum; lane 7, control rabbit serum; lane 8, 200-fold excess of cVitERE oligonucleotide; lane 9, 200 fold excess of hOC VDRE oligonucleotide; lane 10, control rabbit serum; lane 11, anti-RXRα antibody; lane 12, anti-RXRγ antibody.

revealed by chemiluminescent detection (Amersham, Arlington Heights, IL).

3. Results

When the hOC element was used in the electrophoretic mobility shift assay with partially purified canine intestinal extracts, a tissue known to express the VDR protein in relatively high concentrations, two principal bands, B1 and B2, appeared in addition to several weaker, slower-migrating bands (Fig. 1A, lanes 1–4). Specificity for the vitamin D receptor was established by the ability of the monoclonal 9A7γ anti-VDR antibody to disrupt binding and successful cold competition with an excess of unlabeled hOC oligonucleotide as opposed to an unrelated estrogen response element from the chicken vitellogenin II (cVitERE) gene. A nonspecific band did appear under these conditions that failed to interact with the antibody or compete with an excess of unlabeled hOC oligonucleotide (marked by an asterisk, Fig. 1A). The same pattern of binding was observed when the response element identified from the aPTH gene was used in the shift assay, albeit the amount of bound complex was less robust under these conditions [10]. Western blotting of the partially purified canine preparation revealed the presence of a predominate band at 50 kD (Fig. 1A, lane 5), while Western analysis for the RXRα protein indicated the presence of a 55 kD immunoreactive band as well as several smaller fragments (Fig. 1A, lane 6).

Recombinant hVDR and hRXRα extracts derived from baculovirus infected Sf9 cells were also tested in the mobility shift assay with the hOC VDRE. This combination of proteins produced a simplified pattern of binding that resulted in a single prominent band (Fig. 1B). As reported by Ozono et al. and Liao et al. [4,14], no binding to the radiolabeled probe was observed by the individual recombinant protein extracts (Fig. 1B, lanes 1–2). Specificity was confirmed by inclusion of the 9A7γ monoclonal antibody as well as a recently characterized polyclonal anti-VDR antiserum (Fig. 1B, lanes 4–7). Competition with an excess of the cVitERE oligonucleotide had no effect on the complex while an excess of the specific hOC oligonucleotide completely prevented formation of the radiolabeled band (Fig. 1B, lanes 8 and 9). Confirmation of hRXRα presence in the complex was established by inclusion of a polyclonal anti-RXRα peptide antiserum, while normal serum or a polyclonal anti-RXRγ antiserum had no effect on the complex (Fig. 1B, lanes 10–12). Analogous results were observed for binding by the recombinant proteins to the aPTH VDRE ([21], data not shown).

Due to the simplified pattern of binding, the recombinant extracts were used to test the binding affinity of the heterodimer complex to these response elements. A standard binding reaction was employed using the combination of extracts and the radiolabeled aPTH VDRE. Varying amounts of cold, unlabeled oligonucleotides containing the aPTH and hOC direct repeats were added simultaneously with the radiolabeled probe to each reaction mixture. The products were then separated, and the relative amounts of bound radiolabeled aPTH probe determined and plotted as a function of added competing oligonucleotide. As a control, a mutant aPTH oligonucleotide was evaluated in which double mutations were introduced into the second and third guanines (GG → CC) in the 5′ half of the element (5′ mutaPTH). As seen in Fig. 2, the hOC oligonucleotide was approximately five times more effective at competing for binding to the radiolabeled aPTH probe than the unlabeled aPTH oligonucleotide. The 5′ mutaPTH sequence was ineffective at competing for binding over this concentration range.

Interference footprinting protocols in combination with the mobility shift assay were utilized to examine protein-DNA contacts at single nucleotide resolution. Ethylation interference takes advantage of the ability of ethylnitrosourea to modify the phosphate backbone as well as predominantly the guanine residues [17]. Footprints generated with the partially purified canine intestinal extracts, a tissue known to express the VDR protein, were compared to footprints generated by extracts of recombinant human receptors obtained from insect cells. It should be noted that the hOC VDRE used in the earlier gel shift analysis (Fig. 1) contained a potential AP-1 binding site [4]. It was, therefore, of some interest, particularly with regard to

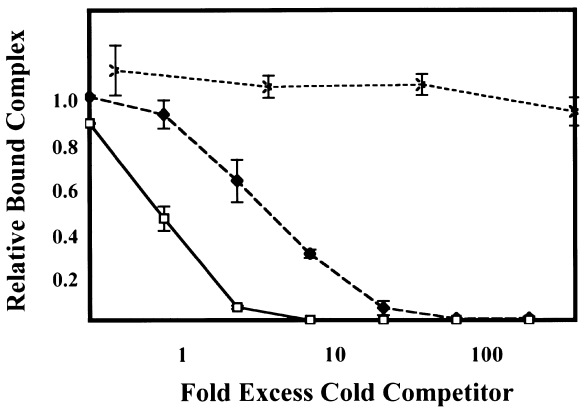

Fig. 2. Cold competition analysis of recombinant proteins binding to the aPTH VDRE. Variable amounts of each competitor were mixed with the radiolabeled aPTH VDRE prior to mixing with the recombinant protein binding reaction. Samples were separated by the mobility shift assay and the amount of bound band remaining was quantitated and normalized versus a control binding reaction with no competitor added. Results presented are from three independent experiments from cold competition experiments using the aPTH (– – –), hOC (—), and 5′mutaPTH (- - - - -) oligonucleotides as shown.

the canine source of VDR that displayed several VDR-containing bands, to determine if the AP-1 site was involved in the observed multiple bound complexes.

The ethylation interference results for the two major bound bands (B1 and B2, Fig. 1) from the canine intestinal preparations for the hOC element are presented in Fig. 3A. The two footprints are essentially the same and show that on the top strand there is significant involvement of the pGpGpG triplet in the 5′ half of the DR + 3 element and, most notably, nearly complete interference over the pGpG dinucleotide sequence corresponding to the first two guanines of the repeat in the 3′ half of this element (Fig. 3A, lanes 1–4). On the opposite strand, strong interference was observed over the pTpGp and the pTpCpA sequences for both complexes (Fig. 3A, lanes 5–8). In addition, no interference was observed over the AP-1 binding site in the B1 and B2 complexes that used the canine intestinal preparation as the source of VDR. Extending the footprinting analysis to two additional, weaker, more slowly migrating complexes failed to reveal any additional footprint areas other than the DR + 3 sequence (data not shown). The combination of recombinant proteins produced only a single bound complex that yielded an interference footprint on both strands that was essentially indistinguishable from that generated by the canine preparation (Fig. 3B).

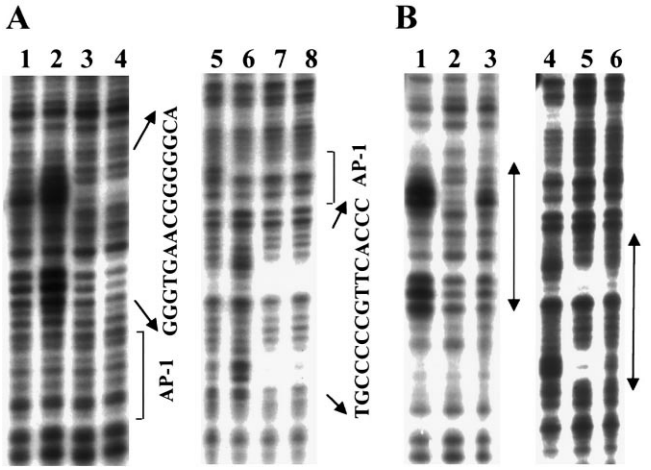

Fig. 3. Ethylation interference footprint analysis of the hOC VDRE. (A) Analysis of B1 and B2 complexes arising from the use of partially purified canine intestinal extract is shown. Footprints from the top (lanes 1–4) and bottom (lanes 5–8) strands are depicted. Lanes 1 and 5, control cleavage profiles of the modified probes; lanes 2 and 6, recovered free DNA; lanes 3 and 7, modified probes recovered from the B1 complex; lanes 4 and 8, B2 complex. AP-1 binding site is indicated by bracketed region. (B) Analysis of the bound complex arising from the use recombinant proteins is shown. Footprint analysis of the top (lanes 1–3) and bottom (lanes 4–6) strands are depicted. Lanes 1 and 4, modified probes recovered from the free DNA; lanes 2 and 5, modified probes recovered from the bound complex; lanes 3 and 6, control cleavage profiles of the modified probes. Double-headed arrows correspond to the sequences depicted

The ethylation interference footprint for the aPTH sequence using the recombinant proteins differed dramatically from that observed for the osteocalcin element. Consistent with an earlier report [10], only weak interference was observed over the pGpGpG triplets in the 5′ and 3′ halves of the top strand of the element (Fig. 4). On the opposite strand, the most significant interference was observed over the pTpGpA sequence, with only very weak interactions detected over the pApCpA region. As reported earlier [10], both the B1 and B2 complexes obtained with the canine preparation generated essentially the same footprint pattern as that seen with the recombinant proteins.

Sodium hydroxide cleavage of ethylnitrosourea-treated DNA hydrolyzes both, the modified phosphate backbone positions as well as guanine residues. However, piperidine treatment of the same modification results in the selective cleavage of the modified guanines [18,19], thus permitting examination of the interfering guanine residues alone. Using the recombinant proteins in this analysis, the guanines on the top strand of the hOC element exhibited significant interference in both halves of the direct repeat, with particularly strong contacts evident over the first two guanines comprising the 3′ half of the element (Fig. 5A). The interference also extended into the guanine in the spacer region immediately adjacent to the 3′ half-site. In contrast, the modified guanine triplets on the top strand of both 5′ and 3′ halves of the aPTH element yielded relatively weaker footprints in this analysis, with stronger interference evident in the

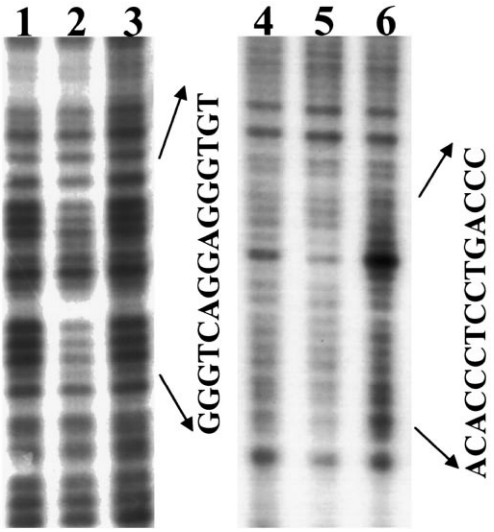

Fig. 4. Ethylation interference footprint analysis of the aPTH VDRE using recombinant proteins in the footprint analysis of the top (lanes 1–3) and bottom (lanes 4–6) strands. Lanes 1 and 4, control cleavage of the modified probes; lanes 2 and 5, modified probes recovered from the bound complex; lanes 3 and 6, modified probes recovered from the free DNA.

guanines comprising the 5′ half-site. On the opposite strands, the only notable interference in the hOC VDRE was seen in the pTpG*cP sequence, while the pTpG*pA was the sole guanine exhibiting interference in the aPTH sequence (data not shown).

To further delineate contacts to individual nucleotides, a thymine interference footprint analysis was also undertaken [20]. On the lower strand of the hOC element, thymine interference was seen in both half-sites and included weak contact with the adjacent thymine in the spacer region (Fig. 5B). No thymine interference note was observed for the top strand of the hOC VDRE (data not shown). In the analysis of the aPTH VDRE, moderately strong interference was observed for the various thymines in both half-sites of the top strand (Fig. 5B), while in the opposite strand the sole interaction occurred in the pT*pGpA sequence (data not shown).

4. Discussion

The partially purified canine intestinal extract produced a complex binding pattern when either the hOC or aPTH response element was used in the mobility shift assay (Fig. 1 and [10]). Although not indicated in Fig. 1, the complex formed with the recombinant proteins migrated most closely to the B2 complex from the canine preparation. Thus, the B1 complex may represent VDR-containing complexes formed with a proteolyzed fragment of a heterodimer partner that still retains the capacity of binding DNA, consistent with the RXRα Western blot showing several smaller protein bands. Alternatively, a different type of heterodimer partner much smaller in size that produces a more quickly migrating complex could also account for the B1 band.

Interference footprinting is predicated based on the concept that chemical modifications to singular positions in a DNA binding site may preclude the ability of a protein to bind to that site, either through steric hindrance or structural perturbations, and thus, be excluded from either bound fraction during the separation procedure. There was excellent agreement in the footprints generated by the partially purified canine intestinal preparation and the recombinant materials obtained from the insect cells for both VDREs. This further confirms the utility of using the recombinant proteins, a more readily available source of large quantities of receptors, for examining the interactions of the VDR/RXR complex with its response elements.

The findings indicated that numerous modified guanines, thymines and phosphate backbone positions within the hOC VDRE were strongly excluded from the bound complex. This was consistent with the methylation interference data reported by others for both, the human and rat osteocalcin gene VDREs [4,11,12], and is highly reminiscent of the footprints observed

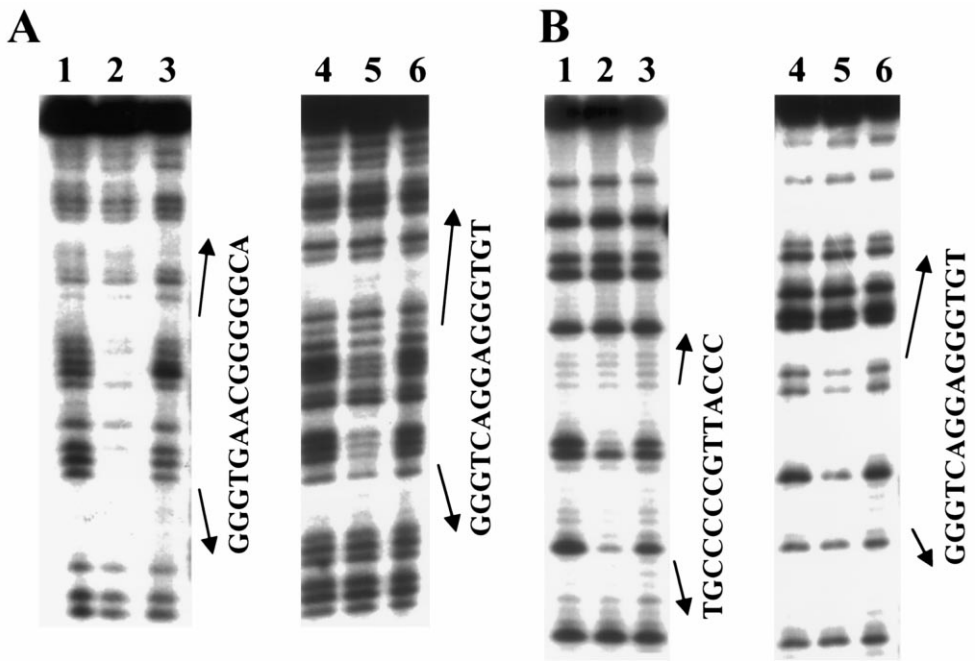

Fig. 5. Guanine and thymine interference profiles of the hOC and aPTH VDREs using recombinant proteins. (A) Guanine interference from ethylated probes for the top strands of the hOC (lanes 1–3) and aPTH (lanes 4–6) VDREs. Lanes 1 and 4, modified probes recovered from free DNA; lanes 2 and 5, modified probes recovered from bound DNA; lanes 3 and 6, control cleavage of modified DNA. (B) Thymine interference for the lower strand of the hOC VDRE (lanes 1–3) and the top strand of the aPTH VDRE (lanes 4–6). Lanes 1 and 4, modified probes recovered from free DNA; lanes 2 and 5, modified probes recovered from bound DNA; lanes 3 and 6, control cleavage of modified DNA.

for the hVDR binding to the murine osteopontin VDRE [13]. There was no difference in the footprints generated by the B1 and B2 complexes from the canine preparations for the hOC VDRE, consistent with the earlier report for the B1 and B2 complexes associated with the aPTH sequence [10]. The present analysis also failed to observe any contact points outside of the recognized hOC DR + 3 VDRE. Additional interference footprints were obtained with the canine extracts from some of the higher order complexes formed with the hOC element immediately above the B2 complex. There was no change in the footprint pattern for these complexes as well (data not shown), indicating that they do not arise from additional protein binding to some other part of the DNA sequence. However, this finding leaves open the possibility of other heterodimer partners, additional protein–protein interactions with other factors [22], or more subtle alterations to the VDR complex resulting in slightly altered mobilities.

Conversely, the same types of modified residues were less likely to be strongly excluded from the bound fraction when the aPTH VDRE was examined. However, paradoxically, the interactions with the aPTH VDRE appeared highly specific with the use of either canine or recombinant sources of receptor proteins [10,21], although a five-fold difference in the ability of this sequence to compete for binding relative to the hOC counterpart was evident (Fig. 2). This suggests that either the heterodimer complex may be making additional contacts with individual cytosine and adenosine nucleotides in the aPTH VDRE not examined in this study or that the bound complex is somehow able to accommodate these uniquely modified positions. Thus, in the aPTH VDRE, any single modification by itself may not be sufficient to entirely block the complex from still binding to that sequence.

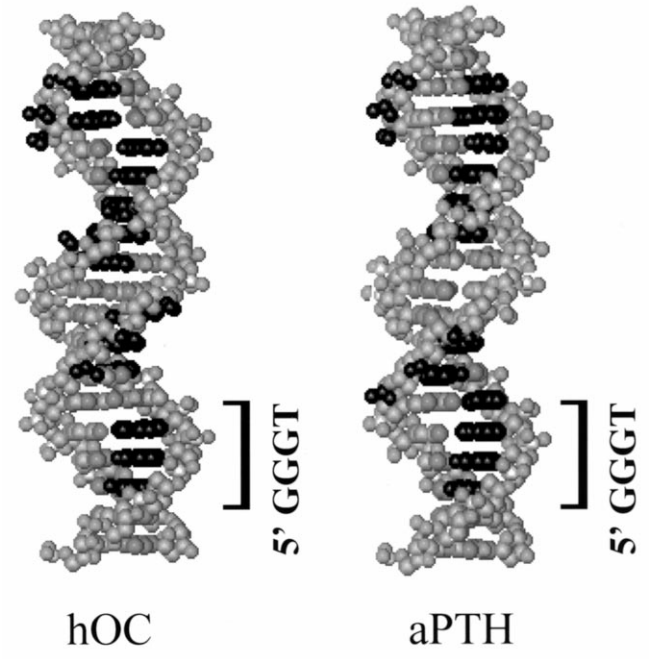

Fig. 6. Summary of interference experiments using the hOC and aPTH VDREs. Helical representations of hOC and aPTH VDREs with all phosphate, guanine and thymine points of interference highlighted in black. Each sequence starts from the bottom of the helix and winds upward.

The footprints were also notable for the degree of contacts made by the complexes within the 3-bp spacer region. On the upper strand of the hOC element, an additional guanine juxtaposed to the 3′ half-site, and on the lower strand a thymine adjacent to the 5′ half-site, exhibited significant interference in these experiments. In contrast, little involvement could be ascribed to the spacer of the aPTH VDRE. However, it should be noted that all of the modified guanine and thymine residues in both half-sites of the aPTH VDRE displayed modest–strong reductions in the bound fraction, suggesting that all were in some way involved in the heterodimer complex binding to this element.

For both the hOC and aPTH sequences, there was a 5′ stagger to the contact points in both halves of the respective response elements, consistent with consecutive major groove binding by the heterodimer complexes (Fig. 6). From the helical representation, it is readily apparent that the greatest differences in the interference profiles generated by this analysis were in the 3′ half-sites of the two respective VDREs. Strong interference with the phosphate backbone and the corresponding guanine and thymines was readily evident in the hOC VDRE over this region, while more limited and overall weaker interactions were detected in the aPTH sequence, particularly with the phosphate positions. The types of interactions occurring over this site may, therefore, be critical in the ultimate response generated by the heterodimer complex. Recent reports indicate that the polarities of VDR/RXR heterodimer complex binding to the hOC and aPTH elements are opposed to each other [21,23]. This is consistent with the present data that indicate much weaker contacts with the aPTH element by the heterodimer, as well as a reduced binding avidity. Thus, the exact sequence of the individual response element may play an active role in defining the transcriptional response by acting as an allosteric modulator of transcriptional activity [24–27]. Consequently, the conformation of the transactivation domains of the heterodimeric complex and the ability to recruit interacting co-factors could be altered as a result of binding to distinct response elements.

Acknowledgements

The authors would like to thank H. Gravatte for

her excellent technical skills in performing the various experiments and L. Tipton for her assistance in preparing the manuscript. This work was supported by National Institutes of Health Grants DK47883 and DK54276 (NJK), DK38422 (JR) and Dialysis Clinic Incorporated (NJK).

References

[1] M.R. Haussler, G.K. Whitfield, C.A. Haussler, J.-C. Hsieh, P.D. Thompson, S.H. Selznick, C.E. Dominguez, P.W. Jurutka, The nuclear vitamin D receptor: biological and molecular regulatory properties revealed, J. Bone Min. Res. 13 (1998) 325–349.

[2] S. Christakos, M. Raval-Pandya, R.P. Wernyj, W. Yang, Genomic mechanisms involved in the pleiotropic actions of 1,25-dihydroxyvitamin D3, Biochem. J. 316 (1996) 361–371 (published erratum appears in Biochem. J. 1996 Sep 15;318 (Pt 3):1079).

[3] M. Noda, R.L. Vogel, A.M. Craig, J. Prahl, H.F. deLuca, D.T. Denhardt, Identification of a DNA sequence responsible for binding of the 1,25-dihydroxyvitamin D3 receptor and 1,25-dihydroxyvitamin D3 enhancement of mouse secreted phosphoprotein 1 (SPP-1 or osteopontin) gene expression, Proc. Natl. Acad. Sci. USA 87 (1990) 9995–9999.

[4] K. Ozono, J. Liao, S.A. Kerner, R.A. Scott, J.W. Pike, The vitamin D responsive element in the human osteocalcin gene. Association with a nuclear proto-oncogene enhancer, J. Biol. Chem. 265 (1990) 21,881–21,888.

[5] C.M. Terpening, C.A. Haussler, P.W. Jurutka, M.A. Galligan, B.S. Komm, M.R. Haussler, The vitamin D responsive element in the rat bone Gla protein gene is an imperfect direct repeat that cooperates with other cis-elements in 1,25-dihydroxyvitamin D3-mediated transcriptional activation, Mol. Endocrinol. 5 (1991) 373–385.

[6] K. Umesono, K.K. Murakami, C.C. Thompson, R.M. Evans, Direct repeats as selective response elements for the thyroid hormone, retinoic acid, and vitamin D3 receptors, Cell 65 (1991) 1255–1266.

[7] C. Zierold, H.M. Darwish, H.F. deLuca, Two vitamin D response elements function in the rat 1,25- dihydroxyvitamin D 24-hydroxylase promoter, J. Biol. Chem. 270 (1995) 1675–1678.

[8] M.B. Demay, J.M. Gerardi, H.F. deLuca, H.M. Kronenberg, DNA sequences in the rat osteocalcin gene that bind the 1,25-dihydroxyvitamin D3 receptor and confer responsiveness to 1,25-dihydroxyvitamin D3, Proc. Natl. Acad. Sci. USA 87 (1990) 369–373.

[9] Y. Ohyama, K. Ozono, M. Uchida, T. Shinki, S. Kato, T. Suda, O. Yamamoto, M. Noshiro, Y. Kato, Identification of a vitamin D responsive element in the 5′-flanking region of the rat 25-hydroxyvitamin D3 24-hydroxylase gene, J. Biol. Chem. 269 (1994) 10545–10550.

[10] S.M. Liu, N. Koszewski, M. Lupez, H.H. Malluche, A. Olivera, J. Russell, Characterization of a response element in the 5′-flanking region of the avian (chicken) PTH gene that mediates negative regulation of gene transcription by 1,25-dihydroxyvitamin D3 and binds the vitamin D3 receptor, Mol. Endocrinol. 10 (1996) 206–215.

[11] E.R. Markose, J.L. Stein, G.S. Stein, J.B. Lian, Vitamin D-mediated modifications in protein-DNA interactions at two promoter elements of the osteocalcin gene, Proc. Natl. Acad. Sci. USA 87 (1990) 1701–1705.

[12] P.N. MacDonald, C.A. Haussler, C.M. Terpening, M.A. Galligan, M.C. Reeder, G.K. Whitfield, M.R. Haussler, Baculovirus-mediated expression of the human vitamin D receptor. Functional characterization, vitamin D response element and interactions, and evidence for a receptor auxiliary factor, J. Biol. Chem. 266 (1991) 18808–18813.

[13] N.J. Koszewski, T.A Reinhardt, R.L. Horst, Vitamin D receptor interactions with the murine osteopontin response element, J. Steroid Biochem Mol. Biol. 59 (1996) 377–388.

[14] J. Liao, K. Ozono, T. Sone, D.P. McDonnell, J.W. Pike, Vitamin D receptor interaction with specific DNA requires a nuclear protein and 1,25-dihydroxyvitamin D3, Proc. Natl. Acad. Sci. USA 87 (1990) 9751–9755.

[15] M.E. Sandgren, M. Bronnegard, H.F. deluca, Tissue distribution of the 1,25-dihydroxyvitamin D3 receptor in the male rat, Biochem. Biophys. Res. Commun. 181 (1991) 611–616.

[16] N.J. Koszewski, T.A. Reinhardt, M.C. Langub, H.H. Malluche, R.L. Horst, Selectivity of a C-terminal peptide antiserum for different DNA-binding states of the vitamin D receptor, Arch Biochem Biophys. 349 (1998) 388–396.

[17] U. Siebenlist, W. Gilbert, Contacts between *Escherichia coli* RNA polymerase and an early promoter of phage T7, Proc. Natl. Acad. Sci. USA 77 (1980) 122–126.

[18] N.J. Koszewski, A.C. Notides, Phosphate-sensitive binding of the estrogen receptor to its response elements, Mol. Endocrinol. 5 (1991) 1129–1136.

[19] H. Buning, P.A. Baeuerle, H. Zorbas, A new interference footprinting method for analysing simultaneously protein contacts to phosphate and guanine residues on DNA, Nucleic Acids Res. 23 (1995) 1443–1444.

[20] M. Truss, G. Chalepakis, M. Beato, Contacts between steroid hormone receptors and thymines in DNA: an interference method, Proc. Natl. Acad. Sci. USA 87 (1990) 7180–7184.

[21] N.J. Koszewski, S. Ashok, J. Russell, Turning a negative into a positive: vitamin D receptor interactions with the avian parathyroid hormone response element, Mol. Endocrinol. 13 (1999) 455–465.

[22] C. Zierold, H.F. deLuca, Additional protein factors play a role in the formation of VDR/RXR complexes on vitamin D response elements, J. Cell Biochem. 71 (1998) 515–523.

[23] C.H. Jin, J.W. Pike, Human vitamin D receptor-dependent transactivation in Saccharomyces cerevisiae requires retinoid X receptor, Mol. Endocrinol. 10 (1996) 196–205.

[24] D.B. Starr, W. Matsui, J.R. Thomas, K.R. Yamamoto, Intracellular receptors use a common mechanism to interpret signaling information at response elements, Genes Dev. 10 (1996) 1271–1283.

[25] J.A. Lefstin, J.R. Thomas, K.R. Yamamoto, Influence of a steroid receptor DNA-binding domain on transcriptional regulatory functions, Genes Dev. 8 (1994) 2842–2856.

[26] V. Misra, S. Walter, P. Yang, S. Hayes, P. O'Hare, Conformational alteration of Oct-1 upon DNA binding dictates selectivity in differential interactions with related transcriptional coactivators, Mol. Cell Biol. 16 (1996) 4404–4413.

[27] J. Huang, T.K. Blackwell, L. Kedes, H. Weintraub, Differences between MyoD DNA binding and activation site requirements revealed by functional random sequence selection, Mol. Cell Biol. 16 (1996) 3893–3900.